ANNNI model in a magnetic field. Possible interpretation of the CeSb phase diagram

V. L. Pokrovskiĭ and G. V. Uĭmin

L. D. Landau Institute of Theoretical Physics, USSR Academy of Sciences
(Submtted 19 November 1981)
Zh. Eksp. Teor. Fiz. **82**, 1640–1662 (May 1982)

The phase diagram of the ANNNI (anisotropic next-nearest-neighbor interaction) model is considered in detail at temperatures lower than that of the transition to the ordered phase with the exception of a very small vicinity of the transition. The method employed has made it possible to determine exactly the sequence of the alteration of the magnetic structure near the degeneracy lines of the ANNNI model, as a function of the temperature and of the magnetic field. The stability of the phase diagram is discussed. The predictions of the theory are compared in the last section with the experimental data on the metamagnet CeSb.

PACS numbers: 75.30.Kz, 75.50.Dd

1. INTRODUCTION

The properties of metamagnets with unusually complicated phase diagrams have attracted much attention in the last few years. These substances include compounds of cerium with elements of the fifth group of the periodic table. A particularly interesting and complicated phase diagram is possessed by cerium antimode CeSb (see Refs. 1–5). Structure investigations show that the phases of this substance are made up of ferromagnetic planes whose moments form a one-dimensional periodic structure with a rather long unit cell containing up to 30 atomic layers. The magnetic interactions in the CeSb lattice are due to indirect exchange, which, owing to the close values of the energies of the localized $4f$-shell electrons and the Fermi-surface s-electrons of the semimetallic cerium antimonide, leads to a strongly anisotropic and Ising-like effective exchange (see Refs. 5–7). One can hardly expect the effective radius of these forces to cover much more than one or two nearest neighbors. This raises the question of attributing the long magnetic periods to short-range forces. It is customary to explain this phenomenon as being due to strong degeneracy of the ground state which is a random sequence of ferromagnetic planes. This degeneracy can arise at a certain ratio of the exchange integrals. Weak perturbations lift this degeneracy. Periodic structures with long cells are produced.

Bak and von Böhm[8] described this phenomenon by using an Ising model with interaction of not only the nearest neighbors. They investigated this model by the self-consistent-field method. A shortcoming of this method for our problems is the need for an empirical choice of several exchange constants for the known sequence of experimental structures.

Fisher and Selke[9,10] considered an Ising model with ferromagnetic interaction of the magnetic moment within a layer, and with interaction of the nearest and next-nearest neighbors between the layers. In the literature this model is abbreviated ANNNI (Anisotropic next-nearest neighbor interaction). They initially[9] investigated the ANNNI numerically by the Monte Carlo method, and subsequently used an analytic method suitable for the low-temperature region.[10] In that paper, to which we shall refer hereafter as FS, they obtained exactly the ground state, followed by the energy and structure of the elementary excitations. In the low-temperature region the elementary excitations constitute a practically ideal gas, so that a virial expansion is possible.

In this paper we use a somewhat different approach within the framework of the very same ANNNI model. We propose a strong anisotropy of the exchange constant, assuming the interaction between the planes by much weaker than within the planes.[1)] This permits the use of high-temperature series in terms of the interplanar coupling constants in almost the entire region of existence of the ordered phase. The relative simplicity of the calculations within the framework of our model has made it possible not only to confirm the FS result, but also to solve the more complicated problem of the behavior the same systems in a magnetic field. The present method is the most adequate for the description of weak interaction induced between magnetic planes by thermal fluctuations.

Besides the direct application to metamagnets, the last problem is vital for the description of the properties of intercalated compounds (see the review[11]). These are layered graphite compounds in which layers of imbedded metal alternate with several layers of graphite. It is natural to describe the imbedded atoms with the aid of a lattice-gas model with a fixed chemical potential or a fixed number of particles. This model is known to be equivalent to an Ising model with a nonzero magnetic field. Another complication arises when a comparison is made with magnetic system because the imbedded atoms can occupy several equivalent positions inside the plane, just as in KC_8. Such a system can be described by using the Potts model. It is possible that the same model can explain the spatial joining together of the charge-density waves in quasi-two-dimensional compounds of the $TaSe_2$ type.[12]

We proceed now to describe the ANNNI model. It is specified by the Hamiltonian

$$\mathcal{H}=\mathcal{H}_0+\mathcal{H}_1, \tag{1}$$

$$\mathcal{H}_0=-\sum_{j,\mathbf{r},\mathbf{r}'} I_0(\mathbf{r}-\mathbf{r}')s_j(\mathbf{r})s_j(\mathbf{r}'), \tag{2}$$

 0038-5646/82/050950-12$04.00

$$\mathcal{H}_1 = {}^1/_2 \sum_{r,j,l\neq 0} I_l s_j(\mathbf{r}) s_{j+l}(\mathbf{r})$$
$$= {}^1/_2 \sum_{j,\mathbf{r}} h_j(\mathbf{r}) s_j(\mathbf{r}), \quad h_j(\mathbf{r}) = \sum_{l\neq 0} I_l s_{j+l}(\mathbf{r}), \tag{3}$$

where $s_j(\mathbf{r}) = \pm 1$, the index j pertains to the number of the plane, and $\mathbf{r}$ is the coordinate of the site inside the layer. The Hamiltonians $\mathcal{H}_0$ and $\mathcal{H}_1$ describe the interaplanar and interplanar interactions, respectively. We assume in addition that the "effective" field h_j produced at the spin by the surrounding planes has two exchange-interaction constants, $I_1 = I_{-1}$ and $I_2 = I_{-2}$.

In the sections that follow we obtain, under the previous assumptions concerning the quantity, I_0 ($I_0 \gg I_1, I_2$), as well as in a temperature region not to close to the temperature of the two-dimensional Ising transition (an estimate is given in Sec. 2), exact results on the sequence of the phase alternation on the phase diagram. It will be shown that in a zero field, when the temperature varies from zero to the transition point of the two-dimensional Ising model, the sequence of alternating magnetic phases is infinite. At a fixed nonzero magnetic field, the number of transitions is infinite as before, but their sequence is different.

At zero temperature and zero magnetic field, there exist on the phase diagram two lines of multiphase points with inifinite degeneracy on them; this degeneracy vanishes instantly at nonzero temperature. In a finite magnetic field at $T = 0$ there exist on the phase diagram four multiphase lines that vanish at a finite temperature. At $T \neq 0$, however, there appear three multiphase lines and an infinite set of a triple-point lines.

In Sec. 12 we discuss the experimental results obtained for cerium antimonide and compare them with the theory.

2. PERTURBATION-THEORY SERIES FOR THE FREE ENERGY

Consider the partition function of a layered system described by the Hamiltonian (1):

$$Z = \prod_j \mathrm{Sp}_j \exp\left(-\frac{1}{T}\mathcal{H}_0(j)\right) \exp\left(-\frac{1}{T}\mathcal{H}_1\right). \tag{4}$$

If we disregard for the time being the interaction (3), we obtain a set of noninteracting planes, each with its own order parameter $\overline{s_j(\mathbf{r})} = s_j$. The order parameters introduced by us can obviously take on only two values:

$$s_j = s\sigma_j; \quad \sigma_j = \pm 1.$$

The sequence of values of σ_j along a stack of N planes is, however, arbitrary (2^N-fold degeneracy).

We now expand the exponentials in Eq. (4) in powers of $\mathcal{H}_1/T$:

$$Z = Z_0^N \left(1 - \frac{1}{T}\overline{\mathcal{H}_1} + \frac{1}{2!T^2}\overline{\mathcal{H}_1^2} - \frac{1}{3!T^3}\overline{\mathcal{H}_1^3} + \ldots\right),$$

where $Z_0(T)$ is the partition function of the two-dimensional Ising model. The bar denotes independent statistical averaging in each plane.

For the free energy we obtain

$$F = NF_0 + \overline{\mathcal{H}_1} - \frac{1}{2!T}\langle\mathcal{H}_1^2\rangle + \frac{1}{3!T^2}\langle\mathcal{H}_1^3\rangle - \ldots, \tag{5}$$

where F_0 is the free energy of the two-dimensional Ising model, and the angle brackets denote irreducible mean values or cumulants. The problem reduces to one-dimensional, and the free energy plays the role of the effective Hamiltonian of a one-dimensional system of spins σ_j, the ground state of the Hamiltonian corresponding to a definite temperature-dependent phase state of the substance.

In first order in the small quantity $I_{1(2)}$, the increment ΔF_1 to the free energy NF_0 of the system of independent planes is

$$\Delta F_1 = \overline{\mathcal{H}_1} = N_l s^2 \sum_j \sigma_j (I_1\sigma_{j+1} + I_2\sigma_{j+2}), \tag{6}$$

where N_l is the number of sites in the layer.

Expression (6) can also be rewritten in the form

$$\Delta F_1 = {}^1/_2 N_l \sum_j \bar{s}\bar{h}_j, \quad \bar{h}_j = \sum_{l\neq 0} I_l \bar{s}_{j+l}, \tag{7}$$

where $\bar{h}_j$ is the self-consistent field acting on the average spin in the plane j and produced by the remaining planes. Thus, the principal term in the expansion of the free energy is the usual self-consistent field approximation.

We consider now the second-order contribution. Each factor $\mathcal{H}_1^n$ included in the irreducible mean value $\langle\mathcal{H}_1^n\rangle$ contains a product [see Eq. (3)] $s_j(\mathbf{r})h_j(\mathbf{r})$ of spins belonging to different planes and independently averaged. We represent graphically the product $s_j(\mathbf{r})h_j(\mathbf{r})$ by two close points. The aggregate of all the connected topologically nonequivalent second-order graphs is shown in Fig. 1. The corresponding irreducible mean value $\langle\mathcal{H}_1^2\rangle$ is the form

$$\langle\mathcal{H}_1^2\rangle = {}^1/_4 s^2 \sum_{j_1,j_2} \sum_{\mathbf{r}_1,\mathbf{r}_2} \{\langle\sigma_{j_1}(\mathbf{r}_1)\sigma_{j_2}(\mathbf{r}_2)\rangle\langle h_{j_1}(\mathbf{r}_1)h_{j_2}(\mathbf{r}_2)\rangle$$
$$+\langle\sigma_{j_1}(\mathbf{r}_1)h_{j_2}(\mathbf{r}_2)\rangle\langle\sigma_{j_2}(\mathbf{r}_2)h_{j_1}(\mathbf{r}_1)\rangle + \langle\sigma_{j_1}(\mathbf{r}_1)\sigma_{j_2}(\mathbf{r}_2)\rangle\langle h_{j_1}(\mathbf{r}_1)h_{j_2}(\mathbf{r}_2)\rangle$$
$$+\langle h_{j_1}(\mathbf{r}_1)h_{j_2}(\mathbf{r}_2)\rangle\overline{\sigma_{j_1}(\mathbf{r}_1)}\,\overline{\sigma_{j_2}(\mathbf{r}_2)} + 2\langle\sigma_{j_1}(\mathbf{r}_1)h_{j_2}(\mathbf{r}_2)\rangle\overline{\sigma_{j_2}(\mathbf{r}_2)}\,\overline{h_{j_1}(\mathbf{r}_1)}\}. \tag{8}$$

The contribution corresponding to graph 1a [first two terms of (8)] does not depend on the signs of the layer magnetizations. At the same time the graph 1b (the remainder of $\langle\mathcal{H}_1^2\rangle$) has two free ends. It is consequently proportional to the product of the spontaneous moments of different planes, and its contribution ΔF_2 to the free energy (5) is equal to:

$$\Delta F_2 = -\frac{N_l s^2}{2T}\sum_{\mathbf{r}}\langle\sigma(0)\sigma(\mathbf{r})\rangle \sum_j \bar{h}_j^2 = -\frac{1}{2}N_l\chi\sum_j \bar{h}_j^2, \tag{9}$$

where

$$\chi = \frac{s^2}{T}\sum_{\mathbf{r}}\langle\sigma(0)\sigma(\mathbf{r})\rangle$$

is the susceptibility of the two-dimensional Ising model.

The physical meaning of (9) is the following: the self-

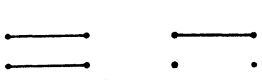

FIG. 1

consistent field changes slightly the moment of each plane, and the energy (9) is due exactly to this change.

Comparing (9) with (7) we see that the high-temperature expansion is valid under the condition

$$\chi I_{1(2)} \ll 1. \tag{10}$$

This condition holds starting with zero temperature up to temperatures separated from the Onsager phase-transition point by an interval of the order of

$$\Delta T \sim T_c (I_1/I_0)^{4/7}. \tag{11}$$

The contribution ΔF_2 to the free energy contains paired products of four types $(\sigma_j\sigma_{j+1}, \sigma_j\sigma_{j+2}, \sigma_j\sigma_{j+3}, \sigma_j\sigma_{j+4})$ with order coefficients $\chi I_1^2 \ll I_1$. In this small contribution it is necessary to take into account only that part of $\Delta F_2'$ whose effective radius exceeds the effective radius of the self-consistent field, i.e., exceeds two:

$$\Delta F_2' = -N_1 s^2 (\chi I_2) \sum_j (2I_1\sigma_j\sigma_{j+3} + I_2\sigma_j\sigma_{j+4}). \tag{12}$$

The remaining terms lead to a small renormalization of the coefficients in (6).

We proceed now to third-order perturbation theory. *Figure 2* shows four types of connected graphs that depend on the signs of the layer magnetizations. The contribution corresponding to Fig. 2a is special. It contains spin couplings of the type $\sigma_j\sigma_{j+5}$ and $\sigma_j\sigma_{j+6}$, which were missing from the preceding order. Their contribution to the free energy is

$$\Delta F_3' = N_1 s^2 (\chi I_2)^2 \sum_j (3I_1\sigma_j\sigma_{j+5} + I_2\sigma_j\sigma_{j+6}). \tag{13}$$

Direct calculation shows that the spin-interaction radius generated by the contributions of the other graphs of Fig. 2 does not exceed four. Allowance for them will lead therefore only to a small deformation of the phase diagram, without changing it qualitatively.

To determine the phase diagram of the considered model it suffices to know the sequence of the longest-range spin couplings. This sequence is easy to calculate. In first, second and third orders it is given in Eqs. (6), (12), and (13). In the n-th order of the high-temperature series we obtain

$$\Delta F_n' = N_1 s^2 (-\chi I_2)^{n-1} \sum_j (nI_1\sigma_j\sigma_{j+2n-1} + I_2\sigma_j\sigma_{j+2n}), \quad n \geqslant 1. \tag{14}$$

3. GROUND STATE OF THE ANNNI MODEL IN A ZERO MAGNETIC FIELD

We shall show here how to minimize in succession the free energy (5). The first step is to find the ground-state structure of the ANNNI model.

Consider the first order of the free-energy expansion (6). In the absence of a magnetic field it is convenient to change from the spin set $\{\sigma_j\}$ to new coupling variable

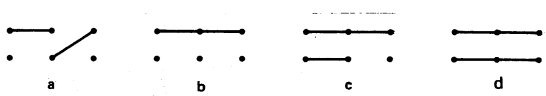

FIG. 2.

$\{\tau_j\}$: $\tau_j = \sigma_j\sigma_{j+1}$, which take on, just as σ_j, two sets of values (± 1). In the new variables, Eq. (6) becomes

$$\Delta F_1 = N_1 s^2 \sum_j (I_1\tau_j + I_2\tau_j\tau_{j+1}). \tag{15}$$

It is necessary next to determine which arrangement of the τ_j couplings along the stack of planes minimizes ΔF_1. We note that to this end it suffices to know the probabilities of the appearance of all possible combinations of couplings between neighboring planes. The number of these combinations is four: $++$, $+-$, $-+$, and $--$. The total energy of an arbitrary configuration of all the interplanar couplings is

$$\Delta F_1 = N_1 s^2 (I_1(N_+ - N_-) + I_2(N_{++} + N_{--} - N_{+-} - N_{-+})). \tag{16}$$

Here $N_+(N_-)$ is the number of positive (negative) couplings between the planes, and N_{++}, N_{+-}, N_{-+}, N_{--} are the numbers of the corresponding pairs of neighboring couplings. Obviously, these numbers, referred to the total number N of the planes determine the probabilities of the appearance of definite couplings or pairs of couplings between the planes. We shall denote hereafter the probability of some configuration by the symbol of this configuration in parentheses, e.g. (+), (+−), etc.

Not all the probabilities defined above are independent. They are obviously connected by the relations

$$(+)+(-)=1, \tag{17}$$

$$(+)=(++)+(+-)=(++)+(-+), \tag{18}$$

$$(-)=(--)+(-+)=(--)+(+-). \tag{19}$$

It follows from (18) and (19) that

$$(+-)=(-+). \tag{20}$$

In addition, the probability normalization condition (17) yields the relation

$$(++)+2(+-)+(--)=1. \tag{21}$$

Thus, out of the six probabilities considered above, only two are independent. It is convenient to choose them to be

$$(++)=p, \quad (--)=q. \tag{22}$$

It follows then from (20) and (21) that

$$(+-)=(-+)=(1-p-q)/2, \tag{23}$$

and from (18) and (19) we can determine the probabilities of the individual couplings:

$$(+)=(1+p-q)/2, \quad (-)=(1-p+q)/2. \tag{24}$$

We shall need later an expression for ΔF_1 in terms of p and q:

$$f_1 = \Delta F_1/N_1 N = (J_1+2J_2)p + (2J_2-J_1)q, \tag{25}$$

where $J_{1(2)} = I_{1(2)} s^2$.

The problem was thus reduced to minimization of a linear function of the variables p and q. The range of these variables is limited by inequalities that follow from (22) and (23)

$$p+q \leqslant 1, \quad p \geqslant 0, \quad q \geqslant 0. \tag{26}$$

This region is the triangle shown in Fig. 3. The function f_1 has at the vertices of this triangle, with coordi-

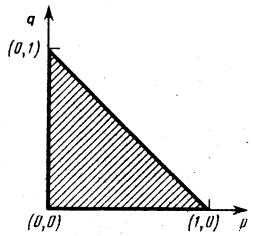

FIG. 3.

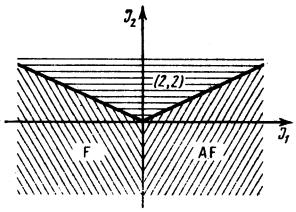

FIG. 4.

nates (p, q) equal to (0, 0), (0, 1), and (1, 0). Each point can be set in correspondence with an ordered phase. Thus, "ferro" ordering of positive couplings corresponds to the point (1, 0). The same ordering but of negative couplings corresponds to the point (0, 1). Finally, at the point (0, 0) we have an "antiferro" ordering of the couplings. In the language of the usual spins, the structure $+++\cdots$ corresponds to the ferromagnetic state $\uparrow\uparrow\uparrow\cdots$ or $\downarrow\downarrow\downarrow\cdots$ (the F phase). In the case of the structure $--\,-\cdots$ we obtain an antiferromagnetic ordering of the spins (AF), $\uparrow\downarrow\uparrow\downarrow\cdots$. Finally, the most interesting phase [(2, 2) in the FS notation] corresponds to the structure $+-\,+-\cdots$.

To determine the region of the existence of each phase, we substitute the values of the probabilities at the corner points in relation (25). Table I lists the values of the free energy, reckoned from the energy of the (2, 2) phase.

Comparison of the energies f_1 allows us to determine the phase diagram of the ANNNI model on the (J_1, J_2) plane (Fig. 4).

We shall show that the phase separation lines $J_2 = |J_1|/2$ on Fig. 4 are infinitely degenerate. We consider for the sake of argument the half-line $J_2 = -J_1/2 (J_1 < 0)$ on which the phases (2, 2) and F coexist.

Indeed, it is seen from (25) that on this line the minimum of f_1 is reached at $(--) = q = 0$ and at arbitrary $p = (++)$ in the interval $0 \leq p \leq 1$. The remaining probabilities are easily expressed in terms of p:

$$(+-) = (-+) = (1-p)/2, \quad (+) = (1+p)/2, \quad (-) = (1-p)/2. \quad (27)$$

Thus, along the line $J_1 + 2J_2 = 0$ $(J_1 < 0)$ the same energy is possessed by all the τ_j configurations that do not contain the element $--$, or by all the σ_j configurations that do not contain the combinations $\uparrow\downarrow\uparrow$ and $\downarrow\uparrow\downarrow$. Such a high degree of degeneracy makes the structure unstable to free-energy increments containing more remote couplings. We know these increments to arise in the next orders of the high-temperature expansion [Eq. (14)]. They lead to the appearance of new structures with long periods in a low vicinity of the degeneracy line. We shall analyzing the splitting of this line in the next section.

TABLE I.

Phase	f_1
(2,2)	0
F	$2J_2+J_1$
AF	$2J_2-J_1$

A similar degeneracy takes place on the line $J_1 - 2J_2 = 0$ $(J_1 > 0)$. The situation is different on the equilibrium line of the F and AF phases: $J_1 = 0$, $J_2 \leq 0$. On this line $p + q = 1$ and consequently $(+-) = (-+) = 0$. The remaining probabilities are expressed in terms of p:

$$(+) = (++) = p, \quad (-) = (--) = 1-p.$$

In this case we have degeneracy in the variable p. Since, however, $(+-) = (-+) = 0$, the configurations that correspond to this degeneracy constitute a two-phase system in which macroscopic pieces of the phases F and AF are separated by a flat boundary. Since there is no continuous degeneracy on this boundary, the contributions of the next higher orders produce only a slight shift of the equilibrium line of these phases.

4. SPLITTING OF DEGENERACY LINES IN A ZERO MAGNETIC FIELD

In a small vicinity of the degeneracy line $J_1 + 2J_2 = 0$ $(J_1 < 0)$ the minimum of the free energy will correspond as before to $q = 0$. Therefore the free energy f can be expressed in first order in the form [see (25)]

$$f = \xi p, \quad (28)$$

where $\xi = 2J_2 + J_1$. Positive ξ correspond to $p = 0$, i.e., to the (2, 2) phase, and negative to $p = 1$, i.e., to the F phase.

We shall consider the substantial contribution F_2 to the free energy in the second order of the high-temperature expansion

$$F_2 = -N_i(\chi I_2) \sum_j (2J_1\tau_j\tau_{j+1}\tau_{j+2} + J_2\tau_j\tau_{j+1}\tau_{j+2}\tau_{j+3}). \quad (29)$$

We must now introduce the probabilities of different configurations comprising groups of three and four successive couplings. Since $q = 0$, only the probabilities of the following triads (+++), (++−), (+−+), (−++), (−+−) differ from zero. These five quantities and the pair probabilities are connected by the four obvious relations

$$(++-) + (+++) = (-++) + (+++) = (++) = p,$$
$$(++-) + (-+-) = (+-) = (1-p)/2, \quad (+-+) = (+-) = (1-p)/2. \quad (30)$$

It is clear therefore that there is only one independent probability of some one triad. It is convenient to introduce as the independent probability $(+++) \equiv r$. All the remaining triad probabilities are easily expressed in terms of p and r:

$$(++-) = (-++) = p-r, \; (+-+) = (1-p)/2, \; (-+-) = (1-3p+2r)/2. \quad (31)$$

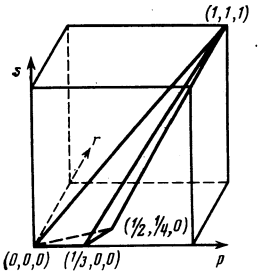

FIG. 5.

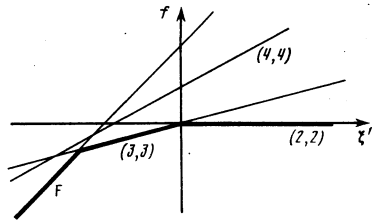

FIG. 6.

A similar analysis for the tetrad probabilities shows that we must introduce one more independent variable, which we choose to be $(++++)=s$. The nonzero probabilities of the remaining tetrads are:

$$(+++-)=(-+++)=(+++)-(++++)=r-s,$$
$$(-++-)=(++-)-(+++-)=p-2r+s, \qquad (32)$$
$$(++-+)=(+-++)=p-r, \quad (+-+-)=(-+-+)=(1-3p+2r)/2.$$

We write down now the contribution (29), of interest to us, to the free energy per lattice site, in terms of the variables introduced by us,[2]:

$$f_2=-2(\chi I_2)\,[-(3J_1+2J_2)p+4J_1r+2J_2s]+\text{const.}$$

Thus, in the 3-dimensional space of the variables (p, r, s) the free energy in the vicinity of the coexistence line of the phases F and (2,2) takes the form

$$f=\xi' p+a(4r-s), \quad a=\chi I_1 J_1, \qquad (33)$$

where ξ' is the deviation, renormalized by a quantity of the order of χJ_1^2, from the interphase boundary $\xi=0$. The free energy is now a function of two parameters. The first (a) is not zero near the degeneracy line and remains practically costant. The parameter ξ' reverses sign on going through the degeneracy line. Therefore, by finding all the corner points of the manifold (p, r, s) we can determine the free energies of all the stable phases as functions of ξ' at fixed a.

To determine the corner points we must solve simultaneously inequalities that follow from Eqs. (32):

$$p\geqslant r\geqslant s\geqslant 0, \quad p-2r+s\geqslant 0, \quad 3p-2r\leqslant 1. \qquad (34)$$

The region defined by inequalities (34) is shown in Fig. 5. It has four corner points. The phases corresponding to these points, the ordering of the couplings and spins, as well as their energies (33) are given in Table II.

Figure 6 shows the free energy the four extremal phases as a function of ξ'. It is easily seen that the coexistence line of the phases (2,2) and F is split and an intermediate phase (3,3) appears in the gap between its two parts. The width $\Delta\xi'$ of the region of its existence is $4a=4\chi I_1 J_1$ and depends on the temperature in the same manner as the susceptibility χ.

In the next higher order we must investigate the equilibrium lines of the phase pairs F– (3,3) and (3,3)–(2,2). On the first line there is a first-order transition since the probability $(+++-)=0$. It remains to ascertain what happens on the (3,3) – (2,2) equilibrium line. Just as in the investigation of the ground state, it can be shown that the (3,3)–(2,2) equilibrium line is an infinite-degeneracy line. The same energy is possessed by all the configurations with $q=r=s=0$, i.e., those in which there are no sections with two adjacent negative and three adjacent positive couplings. This degeneracy is lifted by the terms of the next perturbation-theory order.

Successive application of perturbation theory leads to the following result.[3)] In the m-th step, the degenerate line is the equilibrium line of the phases (2,2) and $(3, 2^m)$ in the FS notation. The unit cell of the $(3,2^m)$ phase consists of a triad of spins of equal directions and of m dyads of spins in the case of odd m:

$$\uparrow\uparrow\uparrow\underbrace{\downarrow\downarrow\uparrow\uparrow\cdots\downarrow\downarrow}_{m\text{ pairs}}.$$

In the case of even m the cell is doubled. In the next step, this line is split. In the gap of width $\sim(\chi I_2)^{m+2}J_1$ there is produced the phase $(3, 2^{m+1})$. The equilibrium lines of the phases $(3, 2^m)$ and $(3, 2^{m+1})$ are first-order transition lines.

The (ξ, T) plane has a multicritical point $\xi=T=0$ from which an infinite number of first-order transition lines emerge and condense towards the line that bounds the region of existence of the (2,2) phase (Fig. 7). The sequence of phase transitions upon variation of ξ is the following:

$$F\to(3,3)\to(3,2)\to(3,2^2)\to\cdots\to$$
$$\to(3,2^m)\to\cdots\to(2,2).$$

These results were first obtained by FS using a somewhat different method.

We point out also that an analysis of the splitting of the degeneracy lines of the phases AF and (2,2) re-

TABLE II.

(p, r, s)	Phase	Coupling sequence	Spin sequence	f
(0, 0, 0)	(2,2)	+−+−⋯	↑↑↓↓⋯	0
(1, 1, 1)	F	+++⋯	↑↑↑⋯ or ↓↓↓⋯	ξ′+3a
(1/3, 0, 0)	(3,3)	++−++−⋯	↑↑↑↓↓↓⋯	ξ′/3
(1/2, 1/4, 0)	(4,4)	+++−⋯	↑↑↑↑↓↓↓↓⋯	ξ′/2+a

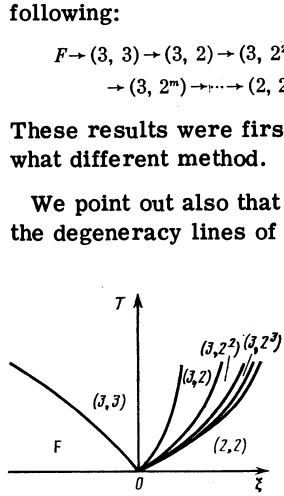

FIG. 7.

duces to the foregoing analysis by making the substitution $J_1 \to -J_1$ and reversing the signs of all the τ_j couplings. The free energy is invariant to this transformation.

5. PHASE DIAGRAM IN A MAGNETIC FIELD. FIRST-ORDER PERTURBATION THEORY

We assume the external magnetic field H to be weak ($H \ll T$) and include it in the Hamiltonian component $\mathcal{H}_1$ used to construct the perturbation theory:

$$\mathcal{H}_1 = {}^1/_2 \sum_{j,r} s_j(\mathbf{r}) h_j(\mathbf{r}) - \sum_{\mathbf{r}} s_j(\mathbf{r}) H. \qquad (3')$$

In first-order perturbation theory, the only term of the expansion of the effective Hamiltonian (i.e., of the free energy) in terms of the field is

$$F_h = -N_1 H \sum_j \bar{s}_j = -N_1 h \sum_j \sigma_j, \quad h = Hs. \qquad (35)$$

All the remaining perturbation-theory terms containing h can generally speaking be comparable in magnitude with those in which h is replaced by h_j. They have, however, a smaller effective radius, and are therefore of no importance. Only in the limit of a strong magnetic field ($h \gg J_1, J_2$) does our reasoning become incorrect. But in such magnetic fields only the ferromagnetic state remains on the phase diagram.

We begin with the case of "moderate" fields:

$$T \gg h \gg (\chi I_1) J_1. \qquad (36)$$

In this case it is necessary to introduce into the first-order effective Hamiltonian the field correction (35), Then

$$F_1 = N_1 \sum_j (-h\sigma_j + J_1 \sigma_j \sigma_{j+1} + J_2 \sigma_j \sigma_{j+2}). \qquad (37)$$

The method of finding the ground state of the effective Hamiltonian (37) is the same as before. The magnetic field, however, violates the symmetry of all spins relative to inversion. We must therefore consider the probabilities of sequences of spins, and not of couplings, so that the space dimensionality of the configurations investigated in a given order increases. Naturally, when considering the ground state of the effective Hamiltonian we must use the probabilities of spin sequences of length not larger than three. Expression (37) is rewritten with the aid of these probabilities as follows:

$$f = F_1/NN_1 = -h((\uparrow) - (\downarrow)) + J_1((\uparrow\uparrow) + (\downarrow\downarrow) - (\uparrow\downarrow) - (\downarrow\uparrow))$$
$$+ J_2((\uparrow\uparrow\uparrow) + (\uparrow\downarrow\uparrow) + (\downarrow\uparrow\downarrow) + (\downarrow\downarrow\uparrow) - (\uparrow\uparrow\downarrow) - (\uparrow\downarrow\downarrow) - (\downarrow\uparrow\uparrow) - (\downarrow\downarrow\downarrow)), \qquad (38)$$

where the symbols in the parentheses denote the probabilities of the corresponding sequences.

Four of the eight probabilities of three-spin sequences are independent. It is convenient to choose them to be

$$(\uparrow\uparrow) = p, \quad (\downarrow\downarrow) = q, \quad (\uparrow\uparrow\uparrow) = r, \quad (\downarrow\downarrow\downarrow) = s. \qquad (39)$$

All the remaining probabilities are expressed in terms of p, q, r, and s:

$$(\uparrow\downarrow) = (\downarrow\uparrow) = (1 - (\uparrow\uparrow) - (\downarrow\downarrow))/2 = (1-p-q)/2, \qquad (40)$$

$$(\uparrow) = (\uparrow\downarrow) + (\uparrow\uparrow) = (1+p-q)/2, \quad (\downarrow) = (1-p+q)/2; \qquad (41)$$

$$(\uparrow\uparrow\downarrow) = (\downarrow\uparrow\uparrow) = (\uparrow\uparrow) - (\uparrow\uparrow\uparrow) = p - r, \quad (\downarrow\downarrow\uparrow) = (\uparrow\downarrow\downarrow) = q - s, \qquad (42)$$

$$(\uparrow\downarrow\uparrow) = (\uparrow\downarrow) - (\uparrow\downarrow\downarrow) = (1-p-3q+2s)/2, \quad (\downarrow\uparrow\downarrow) = (1-3p-q+2r)/2.$$

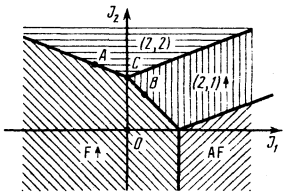

FIG. 8.

The free energy (38) per lattice site is given, apart from an inessential constant, by

$$f = -h(p-q) + 2(J_1 - 2J_2)(p+q) + 4J_2(r+s). \qquad (43)$$

From the definition of the probabilities (39)–(42) follow the inequalities:

$$p \geqslant r \geqslant 0, \quad q \geqslant s \geqslant 0, \quad 3p+q-2r \leqslant 1, \quad 3q+p-2s \leqslant 1. \qquad (44)$$

It is at the corner points of the manifold (p, q, r, s) that we must seek the extremal values of the energy. It is not difficult to find all the corner points, of which there are six:

(0, 0, 0, 0) – the phase AF;

(1, 0, 1, 0)and(0, 1, 0, 1) –the phases F↑ and F↓;

($^1/_3$, 0, 0, 0) and (0, $^1/_3$, 0, 0) – the phases (2, 1)↑and(2, 1)↓;

($^1/_4$, $^1/_4$, 0, 0) – the phase (2, 2).

The arrows indicate here the directions of the total moment. The structure of the state (2, 1) is ... ↑↑↓↑↑↓....

Not all the corner points are on a par. Obviously, we can disregrad the phases F↓ and (2, 1)↓ at $h > 0$, since their energies are always higher than the energies of the phases F↑ and (2, 1)↑, respectively. For a fixed magnetic field $h > 0$ the phase diagram takes in the first order of the high-temperature expansion the form shown in Fig. 8. Comparing the diagram of Fig. 8 with the phase diagram for zero magnetic field (Fig. 4) we can discern the following changes. The ferromagnetic phase extends over a larger region. The equilibrium line of the phases (2, 2) and AF split in two and phase (2, 1) appeared in the resultant gap. A new equilibrium line of the phases F and (2, 1) appeared. The equilibrium lines are described in this approximation by the equations

$$J_1 + 2J_2 = h \ (J_1 < 0); \ \mathrm{F} - (2,2), \qquad (45)$$

$$J_1 + J_2 = h/2 \ (J_1 > 0, \ J_2 > 0); \ F - (2,1), \qquad (46)$$

$$J_1 - 2J_2 = -h \ (J_1 > 0); \ (2,1) - (2,2), \qquad (47)$$

$$J_1 - 2J_2 = h/2 \ (J_2 > 0); \ \mathrm{AF} - (2,1). \qquad (48)$$

6. EQUILIBRIUM LINES OF THE PHASES AF AND (2, 1)↑

We shall show that the AF–(2, 1)↑ phase coexistence line is not split. Along the line joining the corner points corresponding to the phases AF and (2, 1)↑ we have $r = q = s = 0$ and the nonzero probabilities (39) and (42) are given by

$$(\uparrow\uparrow\downarrow) = (\downarrow\uparrow\uparrow) = p, \quad (\uparrow\downarrow\uparrow) = (1-p)/2, \quad (\downarrow\uparrow\downarrow) = (1-3p)/2. \qquad (49)$$

With the aid of (49) it is easy to find the probabilities of the successive spin tetrads:

TABLE III.

Phase	(p, t)	f
AF	(0, 0)	0
$(2,1)\uparrow$	$(1/3, 1/3)$	$(\xi+a)/3$
$(2,1^3)\uparrow$	$(1/5, 0)$	$\xi/5$

$$(\downarrow\uparrow\uparrow\downarrow)=(\uparrow\uparrow\downarrow\uparrow)=(\uparrow\downarrow\uparrow\uparrow)=p, \quad (\uparrow\downarrow\uparrow\downarrow)=(\downarrow\uparrow\downarrow\uparrow)=(1-3p)/2. \tag{50}$$

An additional variable t is needed when the probabilities of five-spin sequences are considered

$$\begin{gathered}(\uparrow\uparrow\downarrow\uparrow\uparrow)=t, \quad (\uparrow\uparrow\downarrow\uparrow\downarrow)=(\downarrow\uparrow\downarrow\uparrow\uparrow)=p-t, \quad (\uparrow\downarrow\uparrow\downarrow\uparrow)=(1-3p)/2,\\ (\uparrow\downarrow\uparrow\uparrow\downarrow)=(\downarrow\uparrow\uparrow\downarrow\uparrow)=p, \quad (\downarrow\uparrow\uparrow\downarrow\downarrow)=(1-5p+2t)/2.\end{gathered} \tag{51}$$

Using second-order perturbation theory we obtain, as before, the free energy in the form of a linear function of the variables p and t:

$$f=\xi p+at.$$

Here

$$a=-4(\chi I_2)J_2<0, \quad \xi=J_1-2J_2-h/2+O(\chi I_1^2).$$

The set of probabilities (51) determines the following inequalities that p and t must obey:

$$p\geqslant t\geqslant 0, \quad 5p-2t\leqslant 1.$$

These in turn lead to the corner points (p, t) given in Table III. The phase $(2, 1^3)\uparrow$ is periodic with a period equal to five: $\ldots\uparrow\uparrow\uparrow\uparrow\downarrow\ldots$. The dependences of f on ξ are given in the last column of Table III, from which it follows than in this order there is no splitting of the phase-coexistence line, although an additional degeneracy parameter did appear. All the orders that follow yield nothing because it is found that $p=t$ already in the second order of the free-energy expansion. This means that the probability $(\uparrow\uparrow\uparrow\uparrow\uparrow)=0$, i.e., the transition from the $(2, 1)\uparrow$ structure into AF is of first order.

7. THE (2, 1)↑–(2, 2) EQUILIBRIUM LINE

We investigate now the stability of the $(2, 1)\uparrow$–$(2, 2)$ equilibrium line. On this line we have $(\uparrow\uparrow\uparrow)=(\downarrow\uparrow\uparrow)=(\downarrow\uparrow\uparrow)=0$. According to (39) and (42) it follows therefore that $r=s=0$ and $q+3p=1$. The nonzero probabilities are

$$(\uparrow\uparrow\downarrow)=(\downarrow\uparrow\uparrow)=p, \quad (\uparrow\downarrow\uparrow)=4p-1, \quad (\downarrow\downarrow\uparrow)=(\uparrow\downarrow\downarrow)=1-3p. \tag{52}$$

It is convenient to make the change of variable $p=(1+p')/4$. Then $p'=0$ corresponds to the $(2, 2)$ phase.

The probabilities of spin tetrads and pentads are uniquely expressed in terms of p'. A two-parameter description is needed only for hexads of successive spins. The free energy in second-order perturbation theory is therefore of the form

$$f=\xi p', \quad \xi=2J_2-J_1-h-2(\chi I_1)(J_1-J_2)+o(\chi I_1^2).$$

In this case there exist only two stable phases, $(2, 2)$ at $p'=0$ and $(2, 1)\uparrow$ at $p'=1/3$. Only the third order can lead to a splitting of the degeneracy line. We present below the values of those spin hexad and heptad probabilities which depend on the second variable u on the $(2, 1)\uparrow \rightarrow (2, 2)$ state-degeneracy line:

TABLE IV.

Phase	$(p'u)$	f
(2,2)	(0,0)	0
$(2,1)\uparrow$	$(1/3, 1/3)$	$(\xi+a)/3$
$(2^3, 1)\uparrow$	$(1/7, 0)$	$\xi/7$

$$\begin{gathered}(\uparrow\downarrow\uparrow\uparrow\downarrow\uparrow)=u, \quad (\uparrow\downarrow\uparrow\uparrow\downarrow\downarrow)=(\downarrow\uparrow\uparrow\downarrow\uparrow\uparrow)=p'-u,\\ (\downarrow\uparrow\uparrow\downarrow\downarrow\uparrow)=(\downarrow\uparrow\uparrow\downarrow\uparrow\downarrow)-(\downarrow\uparrow\uparrow\downarrow\downarrow\uparrow)=(\downarrow\uparrow\uparrow)-p'+u=(1-7p'+4u)/4;\end{gathered} \tag{53}$$

$$\begin{gathered}(\uparrow\uparrow\downarrow\uparrow\uparrow\downarrow\uparrow)=(\uparrow\downarrow\uparrow\uparrow\downarrow\uparrow\uparrow)=u, \quad (\uparrow\downarrow\uparrow\uparrow\downarrow\uparrow\downarrow)=(\downarrow\uparrow\uparrow\downarrow\uparrow\uparrow\downarrow)=(1-7p'+4u)/4;\\ (\uparrow\uparrow\downarrow\uparrow\uparrow\downarrow\downarrow)=(\uparrow\downarrow\uparrow\uparrow\downarrow\uparrow\downarrow)=(\uparrow\downarrow\uparrow\uparrow\downarrow\downarrow\uparrow)=(\downarrow\uparrow\uparrow\downarrow\uparrow\uparrow\downarrow)=p'-u.\end{gathered} \tag{54}$$

The inequalities that follow from the definitions (54) of the probabilities,

$$p'\geqslant u\geqslant 0, \quad 7p'-4u\leqslant 1,$$

lead to the corner points for which the data are gathered in Table IV.

The free energy can be written in the form

$$f=\xi p'+au.$$

The coefficient a is found to be positive

$$a=12(\chi I_2)^2 J_1>0.$$

In the spirit of the FS notation, the form $(m_1^{n_1}, m_2^{n_2}, m_3^{n_3}\ldots)$ denotes a periodic spin structure consisting of n_1 groups each with m_1 parallel spins, n_2 groups each with m_2 parallel spins, etc., with the spins of neighboring groups of opposite sign. In particular, the phase $(2^3, 1)\uparrow$ of interest to us has the unit cell $\uparrow\uparrow\uparrow\downarrow\uparrow\uparrow\uparrow\downarrow$.

An analysis of the free energies of the competing phases shows that the equilibrium lines are split. A phase $(2^3, 1)\uparrow$ is produced in the gap between the phases $(2, 1)\uparrow$ and $(2, 2)$. Further analysis shows that a splitting of the equilibrium line of the phases $(2, 2)$–$(2^{2m+1}, 1)\uparrow (m\geqslant 1)$ takes place in the odd orders of perturbation theory. The sequence of the produced phases is

$$(2,1)\uparrow \rightarrow (2^3,1)\uparrow \rightarrow \ldots \rightarrow (2^{2m+1},1)\uparrow \rightarrow \ldots \rightarrow (2,2).$$

Thus, a magnetic field h that satisfies the condition (36) excludes a whole set of $(2^{2m}, 1)$ states having zero magnetization.

8. THE F↑–(2, 2) EQUILIBRIUM LINE

We show now how to derive expressions for the probabilities of various spin sequences along the degeneracy line of the states F↑ and (2, 2). In Sec. 5 we obtained the corner points (p, q, r, s) for the phases F↑ and (2, 2): (1, 0, 1, 0) and (1/4, 1/4, 0,0). A straight line must be drawn through them. This line can be represented as the intersection of the surfaces $s=0$, $q=(1-r)/4$ and $p=(1+3r)/4$.

Thus the single-parameter description of the degeneracy line determines the nonzero probabilities of the three-spin sequences:

$$(\uparrow\uparrow\uparrow)=r, \quad (\uparrow\uparrow\downarrow)=(\uparrow\downarrow\downarrow)=(\downarrow\uparrow\downarrow)=(\downarrow\uparrow\uparrow)=(1-r)/4. \tag{55}$$

TABLE V.

Phase	(r, v, w)	f
(2,2)	(0, 0, 0)	0
F↑	(1, 1, 1)	ξ+a+b
(3,2)↑	(1/5, 0, 0)	ξ/5
(4,2)↑	(1/5, 1/6, 0)	ξ/3+a/6

It is obvious from (55) that, first, that the inverted spins can exist only as isolated pairs. Second, the number of positive spins that separate pairs of negative spins is larger than unity. All these configurations are degenerate in energy.

To determine the probabilities of long spin sequences it is necessary to introduce two more new variables: $(\uparrow\downarrow\uparrow\uparrow)=v$ and $(\uparrow\downarrow\uparrow\uparrow\uparrow)=w$. The remaining probabilities are expressed in terms of r, v, and w:

$$(\uparrow\uparrow\uparrow\downarrow)=(\downarrow\uparrow\uparrow\uparrow)=r-v,\quad (\downarrow\uparrow\uparrow\downarrow)=(1-5r+4v)/4,$$
$$(\downarrow\uparrow\downarrow\uparrow)=(\uparrow\uparrow\downarrow\downarrow)=(\uparrow\downarrow\uparrow\uparrow)=(1-r)/4; \tag{56}$$
$$(\uparrow\uparrow\uparrow\uparrow\downarrow)=(\downarrow\uparrow\uparrow\uparrow\uparrow)=v-w,$$

$$(\uparrow\uparrow\downarrow\downarrow\uparrow)=(\uparrow\downarrow\downarrow\uparrow\uparrow)=(1-r)/4,\quad (\downarrow\uparrow\uparrow\downarrow\downarrow)=(\downarrow\uparrow\uparrow\downarrow\uparrow)=(1-5r+4v)/4,$$
$$(\uparrow\uparrow\uparrow\downarrow\downarrow)=(\downarrow\downarrow\uparrow\uparrow\uparrow)=r-v,\quad (\downarrow\uparrow\uparrow\uparrow\downarrow)=r-2v+w. \tag{57}$$

From the condition that the probabilities (57) be positive we get the inequalities

$$r\geqslant v\geqslant w\geqslant 0,\quad r-2v+w\geqslant 0,\quad 5r-4v\leqslant 1. \tag{58}$$

The corner points of the manifold (r, v, w), obtained with the aid of (58), are represented in Table V. The region of admissible values of r, v, and w is itself an irregular tetrahedron. Table V contains also the energies of the four competing states:

$$f=\xi r+av+bw;$$
$$a=-8(\chi I_2)J_1>0,$$
$$b=-4(\chi I_2)J_2<0, \tag{59}$$
$$\xi=J_1+2J_2-h-2(\chi I_1)(J_1+J_2)+o(\chi I_1^2).$$

When investigating the dependence of f on ξ, a distinction must be made between two variants. In the first $(J_2<2|J_1|)$ [Fig. 9(a)] the equilibrium line of the phases F↑ and (2, 2) is split. A new phase (3, 2)↑ appears in the gap.

In the second case $2|J_1|<J_2$ there is no splitting [Fig. 9(b)]. A first-order transition takes place directly from F↑ to (2, 2). This result is not changed in the subsequent orders of perturbation theory. The structure (4. 2)↑ is always not favored.

We turn now to Fig. 8. The point A on this figure is the intersection of the straight line $J_2=2|J_1|$ with the

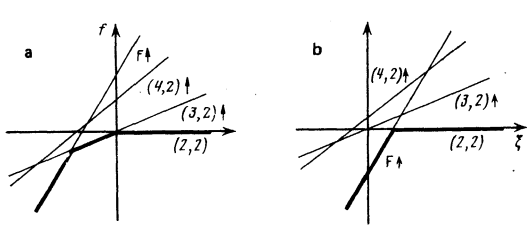

FIG. 9.

F↑–(2, 2) equilibrium line. It can be shown that on the left of the point A the equilibrium line is split into an infinite sequence of states:

$$F\uparrow\to(3,2)\uparrow\to(3,2^2)\uparrow\to\ldots\to(3,2^{2m+1})\uparrow\to\ldots\to(2,2).$$

Consequently a point lying on the line $J_2=2|J_1|$ is multiphase at a magnetic field value $h\approx 3|J_1|$. More accurately speaking, in a nonzero magnetic field there appears a line of multiphase points defined in first order by the equations

$$h=3|J_1|+C_1\chi J_1^2,\quad h=J_1+2J_2+C_2\chi J_1^2.$$

It can be interpreted as a line in the three-dimensional space (P, T, h), where P is the pressure.

9. THE F↑–(2, 1)↑ EQUILIBRIUM LINE

The straight line joining the corner points corresponding to the states F↑ and (2, 1)↑ is specified by the equations

$$q=s=0,\quad 3p-2r=1.$$

This leads to the following spin-triad probabilities

$$(\uparrow\uparrow\uparrow)=r,\quad (\uparrow\uparrow\downarrow)=(\uparrow\downarrow\uparrow)=(\downarrow\uparrow\uparrow)=(1-r)/3. \tag{60}$$

To describe sequences of four and five spins it is necessary to introduce two more variables. We recognize here that only solitary negative spins are encountered, while the positive spins come in groups of not less than two:

$$(\uparrow\uparrow\uparrow\uparrow)=x,\quad (\uparrow\uparrow\uparrow\downarrow)=(\downarrow\uparrow\uparrow\uparrow)=r-x,$$
$$(\uparrow\uparrow\downarrow\uparrow)=(\uparrow\downarrow\uparrow\uparrow)=(1-r)/3,\quad (\downarrow\uparrow\uparrow\downarrow)=(1-4r+3x)/3; \tag{61}$$
$$(\uparrow\uparrow\uparrow\uparrow\uparrow)=y,\quad (\uparrow\uparrow\uparrow\uparrow\downarrow)=(\downarrow\uparrow\uparrow\uparrow\uparrow)=x-y,$$
$$(\uparrow\uparrow\uparrow\downarrow\uparrow)=(\uparrow\downarrow\uparrow\uparrow\uparrow)=r-x,\quad (\uparrow\uparrow\downarrow\uparrow\uparrow)=(1-r)/3, \tag{62}$$
$$(\downarrow\uparrow\uparrow\uparrow\downarrow)=r-2x+y,\quad (\downarrow\uparrow\uparrow\downarrow\uparrow)=(\uparrow\downarrow\uparrow\uparrow\downarrow)=(1-4r+3x)/3.$$

The inequalities imposed on r, x, and y are

$$r\geqslant x\geqslant y\geqslant 0,\quad r-2x+y\geqslant 0,\quad 4r-3x\leqslant 1. \tag{63}$$

Relations (63) and (58) are similar in form. The corner points defined in (63) are given in Table VI, together with the free energy at these points. The latter takes the form

$$f=\xi r+ax+by;$$
$$a=-8(\chi I_2)(J_1-J_2),\quad b=-4(\chi I_2)J_2,$$
$$\xi=4/3[(J_1+J_2-h/2)-(\chi I_1)(2J_2+J_1)].$$

An analysis similar to the foregoing shows that if $J_2>2J_1$ the phase degeneracy line is split, and a structure (3, 1)↑ is formed between the states F↑ and (2, 1)↑. If, however, $J_2<2J_1$, not only (4, 1)↑ but also (3, 1)↑ become energywise unfavored. The transition F↑ → (2, 1)↑ is then of first order ($(\uparrow\uparrow\uparrow\uparrow\uparrow)=0$). Consequently the phase equilibrium line to the right of the point B on Fig. 8 remains continuous in all orders of

TABLE VI.

Phase	(r, x, y)	f
(2.1)↑	(0. 0. 0)	0
F↑	(1. 1. 1)	ξ+a+b
(3.1)↑	(1/4, 0. 0)	ξ/4
(4.1)↑	(2/5, 1/5, 0)	2ξ/5+a/5

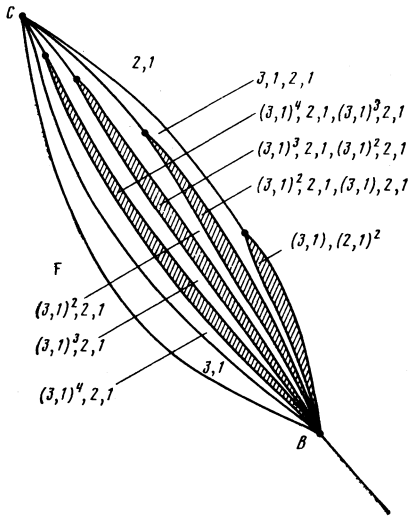

FIG. 10.

perturbation theory. There is also a first order transition between the phases F↑ and (3.1)↑.

Further analysis shows that the (2, 1)↑–(3, 1)↑ phase equilibrium line is split in the following manner: Just as on the F↑–(2, 2) phase coexistence line, the straight line in question has a multiphase point (point B in Fig. 8). There is no splitting on its right, and on the left where is splitting into an infinite sequence of states. The limiting state for them is (3, 1)↑, and the general term of the sequence is $((3,1)^m, 2, 1)\uparrow$. This, however, does not limit the phase diagram in this region: each line that separates phase states, e.g., $((3,1)^m, 2, 1)\uparrow$ and $((3,1)^{m+1}, 2, 1)\uparrow$, is split and a strip of a new phase $((3,1)^m, 2, 1, (3,1)^{m+1}, 2, 1)\uparrow$ is formed. This new phase is bounded on one side by the multiphase point B, and on the other by the triple point with coordinates $J_2 = (4m+5)J_1/2$ and $h = (4m+7)J_1$. Thus, we get an infinite sequence of triple points that converge to the multiphase point C (Fig. 8).

The character of the splitting of the equilibrium line between the multiphase points B and C is shown in Fig. 10.

10. PHASE DIAGRAM IN WEAK MAGNETIC FIELDS

We consider the magnetic-field region bounded by the inequalities

$$J_1 \gg h \gg (\chi I_1)^2 J_1. \tag{64}$$

These fields must be taken into account alongside the second order of perturbation theory. The phase diagram that appears in first-order perturbation theory is changed little by these fields. We have in mind the fact that the produced splittings and displacements of the equilibrium lines are of the order of h. We point out that the region bounded by the inequalities (64) overlaps the previously investigated region of the magnetic fields described by the inequalities (36). In the general case we shall consider magnetic fields whose values are bounded by the relations

$$(\chi I_1)^{m-2} J_1 \gg h \gg (\chi I_1)^m J_1. \tag{65}$$

Such a magnetic field must be taken into account together with the m-th order of perturbation theory. Therefore the phase diagram changes little compared with the contribution of the $(m-1)$st order in the absence of a magnetic field. Each such field region [see (65)] overlaps with the preceding one. Considering ever larger m, we go over continuously to the case $h=0$.

We turn now to the region of magnetic fields bounded by the inequalities (64). We consider as the basis the Hamiltonian

$$\mathcal{H}_1 = \sum_j (J_1\sigma_j\sigma_{j+1} + J_2\sigma_j\sigma_{j+2}). \tag{66}$$

The perturbation now is

$$\mathcal{H}_2 = \sum_j (-h\sigma_j - (\chi I_2)(2J_1\sigma_j\sigma_{j+3} + J_2\sigma_j\sigma_{j+4})). \tag{67}$$

Since $\mathcal{H}_1$ does not contain a magnetic field, the degeneracy lines are, as in Fig. 4 before, the lines $J_1 \pm 2J_2 = 0$. We consider first the line $J_1 + 2J_2 = 0$ $(J_1 < 0)$, where the phases F and (2, 2) compete. The F phase can correspond to positive or negative magnetization. Consequently, we must consider the degeneracy plane of the three states F↑, F↓, and (2, 2). We use the previously determined spin-sequence probabilities [Eqs. (39)–(42)]. In the (p, q, r, s) space the sought plane should pass through the points (1, 0, 1, 0), (0, 1, 0, 1) and $(\frac{1}{4}, \frac{1}{4}, 0, 0)$. The equations that define this plane are

$$p+s=r+q, \quad r+4q=1+3s.$$

We present below a two-parameter representation of the nonzero probabilities of spin triads [cf. Eqs. (39), (42)]:

$$(\uparrow\uparrow\uparrow)=r, \quad (\downarrow\downarrow\downarrow)=s, \quad (\uparrow\uparrow\downarrow)=(\downarrow\uparrow\uparrow)=(\uparrow\downarrow\uparrow)=(\uparrow\downarrow\downarrow)=(1-r-s)/4. \tag{68}$$

To construct the probabilities of four- and five-spin sequences it becomes necessary to introduce two more pairs of variables: $r_1 = (\uparrow\uparrow\uparrow\uparrow)$, $s_1 = (\downarrow\downarrow\downarrow\downarrow)$, $r_2 = (\uparrow\uparrow\uparrow\uparrow\uparrow)$, $s_2 = (\downarrow\downarrow\downarrow\downarrow\downarrow)$. Then

$$\begin{gathered}(\uparrow\uparrow\downarrow\downarrow)=(\downarrow\uparrow\uparrow\downarrow)=(1-r-s)/4, \quad (\downarrow\uparrow\uparrow\uparrow)=(\uparrow\uparrow\uparrow\downarrow)=r-r_1,\\ (\uparrow\downarrow\downarrow\downarrow)=(\downarrow\uparrow\downarrow\downarrow)=s-s_1, \quad (\uparrow\downarrow\uparrow\downarrow)=(1-r-5s+4s_1)/4,\\ (\downarrow\uparrow\uparrow\downarrow)=(1-5r-s+4r_1)/4;\end{gathered} \tag{69}$$

$$\begin{gathered}(\uparrow\uparrow\uparrow\uparrow\downarrow)=(\downarrow\uparrow\uparrow\uparrow\uparrow)=r_1-r_2, \quad (\downarrow\downarrow\downarrow\downarrow\uparrow)=(\uparrow\downarrow\downarrow\downarrow\downarrow)=s_1-s_2,\\ (\uparrow\uparrow\uparrow\downarrow\downarrow)=(\downarrow\uparrow\uparrow\uparrow\downarrow)=r-r_1, \quad (\downarrow\downarrow\downarrow\uparrow\uparrow)=(\uparrow\uparrow\downarrow\downarrow\downarrow)=s-s_1,\\ (\downarrow\uparrow\uparrow\uparrow\downarrow)=r-2r_1+r_2, \quad (\downarrow\uparrow\downarrow\downarrow\downarrow)=(\downarrow\downarrow\uparrow\downarrow\downarrow)=(1-5r-s+4r_1)/4,\\ (\uparrow\downarrow\downarrow\downarrow\uparrow)=s-2s_1+s_2, \quad (\uparrow\downarrow\uparrow\uparrow\uparrow)=(\uparrow\uparrow\downarrow\uparrow\uparrow)=(1-r-5s+4s_1)/4.\end{gathered} \tag{70}$$

It can be verified directly with the aid of Eqs. (66)–(70) that the free energy takes the following general form:

$$f = \xi(r+s) - h(r-s) + a(r_1+s_1) + b(r_2+s_2), \tag{71}$$

where, as before, $\xi = J_1 + 2J_2$ and reverses sign in the vicinity of the degeneracy line, while the coefficients a and b can be obtained from (67) and (69), (70):

$$a = -8(\chi I_2)J_1, \quad b = -4(\chi I_2)J_2 \quad (J_1 < 0).$$

The range of variation of the variables $(r, r_1, r_2; s, s_1, s_2)$ is given by the system of inequalities

$$\begin{gathered}r \geqslant r_1 \geqslant r_2 \geqslant 0, \quad s \geqslant s_1 \geqslant s_2 \geqslant 0,\\ r-2r_1+r_2 \geqslant 0, \quad s-2s_1+s_2 \geqslant 0,\\ 5r+s-4r_1 \leqslant 1, \quad 5s+r-4s_1 \leqslant 1.\end{gathered} \tag{72}$$

TABLE VII.

Phase	$(r, r_1, r_2; s, s_1, s_2)$	f
(2,2)	(0, 0, 0: 0, 0, 0)	0
F↑	(1, 1, 1: 1, 1, 1)	$\xi-h+a+b$
(3,3)	($^1/_6$, 0, 0; $^1/_6$, 0, 0)	$\xi/3$
(3,2)↑	($^1/_5$, 0, 0; 0, 0, 0)	$(\xi-h)/5$
(4,2)↑	($^1/_3$, $^1/_6$, 0; 0, 0, 0)	$(2\xi-2h+a)/6$
(4,3)↑	($^2/_7$, $^1/_7$, 0; $^1/_7$, 0, 0)	$(3\xi-h+a)/7$
(4,4)	($^1/_4$, $^1/_8$, 0; $^1/_4$, $^1/_8$, 0)	$(2\xi+a)/4$

Its corner points, which contribute to the non-negative moment of the state, are listed in Table VII together with their free energies. The three last phases in Table VII are energywise unfavored. Thus, the two inequalities

$$f_{(4,2)}<f_F, \quad f_{(4,2)}<f_{(3,2)}$$

become contradictory at $b<0$. Similar contradictions are revealed by examination of other pairs of inequalities

$$f_{(4,3)}<f_{(3,3)}, \quad f_{(4,3)}<f_F;$$
$$f_{(4,4)}<f_{(3,3)}, \quad f_{(4,4)}<f_F.$$

The remaining four phases form on the (ξ, h) plane the phase diagram shown in Fig. 11. The phase-equilibrium lines in the right-hand half-planes are defined by the equations

$$\xi-h=0, \qquad (2,2)-(3,2)\uparrow,$$
$$\xi-h+5(a+b)/4=0 \quad (h\geqslant h_0), \quad (3,2)\uparrow-F\uparrow,$$
$$\xi+3h/2 \quad (h\leqslant h_0), \qquad (3,3)-(3,2)\uparrow,$$
$$\xi-3h/2+3(a+b)/2=0 \quad (h\leqslant h_0), \quad (3,3)-F\uparrow,$$

where $h_0=(a+b)/2>0$.

Only one of the foregoing phase-equilibrium lines is subject to splitting, namely the line $\xi=h$, where the phases (2.2) and (3.2) are degenerate. But this degeneracy was already considered by us in another range of magnetic fields, $\chi I_1 J_1 \ll h \ll T$. Since both regions overlap, the splitting picture cannot change. It takes place in the same way as the splitting of the F–(2, 2) phase degeneracy line on Fig. 8 to the left of the point A. On the remaining lines the phase transition is of first order, as follows again from the preceding analysis.

A more thorough investigation is needed for the vicinity of the point $h=0$, $\xi=0$. At this point, according to the phase diagram of Fig. 11, there coexist four different phases (2, 2), (3, 2)↓, (3, 2)↑, (3, 3). In the next-order approximation, the phase diagram differs from that in Fig. 11 in the appearance of a small section $\sim(\chi I_1)^2 J_1$ of the equilibrium line of the phases (3, 2)↓ and (3, 2)↑ near $\xi=h=0$, as shown in Fig. 12. Now the phases (2, 2), (3, 2)↓ and (3, 2)↑ compete in the vicinity of the origin. In the next perturbation-theory order, a rhombic region is produced in which the phase $(3, 2^2)$ exists and which borders with the strips of the phases $(3, 2^3)$ and (3. 1) (Fig. 13). In final analysis, the sequence of phases produced near the origin is the same as at $h=0$, but now the nonmagnetic phases occupy only small rhombic regions which are smaller the longer their unit cell.

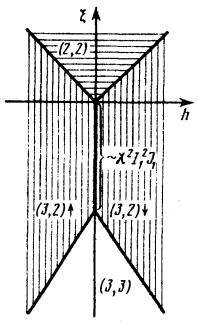

FIG. 12.

The foregoing picture corresponds to the region of small h and to exchange parameters near the half-line $\xi=J_1+2J_2=0$ $(J_1<0)$. We proceed now to investigate the vicinity of the other degeneracy line

$$\eta=-J_1+2J_2=0 \quad (J_1>0).$$

Obviously, the same phase sequence appears in the vicinity of the point $\eta=h=0$ as at $h=0$, i.e., the phases AF, (2, 1), $(2^2, 1)$, ..., $(2^m, 1)$, ..., (2, 2). On the (η, h) plane the regions of existence of nonmagnetic phases (where m are even) are bounded and are rhombs with sides $\sim(\chi I_2)^m J_1$. The result obtained in third-order perturbation theory is shown schematically in Fig. 14.

We call attention to the set of triple points that coincide with the vertices of the rhombs. The limit point of such a set as the point $\xi=h=0$.

11. STABILITY OF PHASE DIAGRAMS

We have investigated the phase diagram of a system with two interplanar couplings were assumed to be of the same order. Inclusion of longer-range interactions

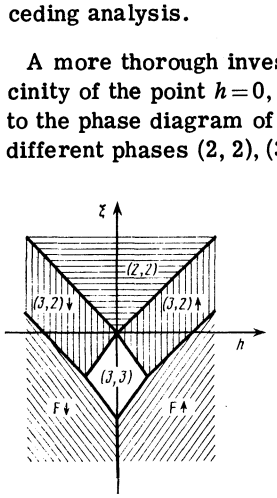

FIG. 11.

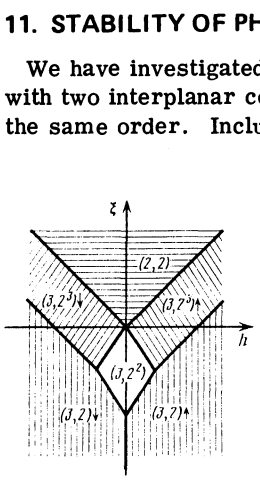

FIG. 13.

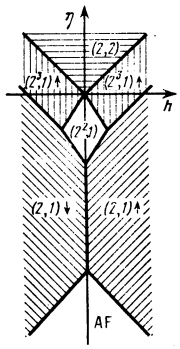

FIG. 14.

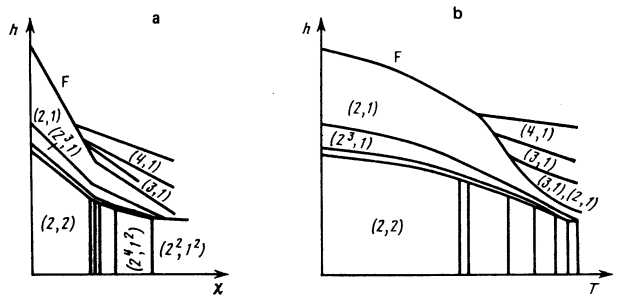

FIG. 15.

in the Hamiltonian (1)–(3) can in principle alter radically the entire phase diagram. In this sense, the diagram is unstable. It is obvious, however, that if the energies of the longer-range couplings are low enough, some of the phase sequences obtained by us remain unchanged.

The direct interplanar bonds $I_k (k \geq 3)$ can be taken into account in the same manner as in a magnetic field, if they are assumed to be small enough. Namely, if the I_k satisfies the inequalities

$$(\chi I_1)^{n+1} I_1 \ll |I_k| \ll (\chi I_1)^{n-1} I_1, \tag{73}$$

such a coupling must be taken into account alongside the n-th order of perturbation theory. The radius of the fluctuation interaction between the planes, which appear in n-th order of the expansion of the free energy, is equal to $2n$. The inequality (73) determines $n(k)$ as a function of k. If $k < 2n(k)-1$, the direct coupling I_k is inessential. In particular, the phase-diagram stability region is determined by the system of inequalities

$$|I_k| \ll (\chi I_1)^{(k-1)/2} I_1.$$

In the case $k > 2n(k)$ the phase diagram, starting with order $n(k)$, changes. If $k = 2n(k)$ or $k = 2n(k)-1$, the phase diagram changes if the direct coupling leads to reversal of the signs of the coefficients of the linear function that represents the free energy.

Obviously, the infinite number of phase transitions predicted by the theory cannot be observed in experiment. The most important hindrance to the appearance of excessively long cells is believed by us to be the presence of fluctuations in which one plane as a whole reverses the direction of its moment. It is always possible to choose this plane such that the free-energy loss per atom is of the order of

$$(\chi I_1)^l J_1,$$

where l is approximately half the length of the unit cell. The total change of free energy in such a fluctuation is

$$\sim N (\chi I_1)^l J_1,$$

where N is the number of atoms in the plane. Comparing this quantity to the temperature, we obtain the maximum length of a cell that is not destroyed by thermal fluctuations:

$$l \sim \ln N / |\ln (\chi I_1)|.$$

The length l does not exceed about forty interplanar layers even at $\chi I_1 \sim 1$.

12. POSSIBLE INTERPRETATION OF THE CeSb PHASE DIAGRAM

Even very simple elaborations of the picture described above, such as small direct couplings between third and fourth neighbors, give rise to a rather cumbersome, albeit not complicated, picture of the phase diagram. Without presenting it completely, we consider only the case when I_3 and I_4 satisfy the following system of inequalities:

$$\begin{aligned} &(\chi I_1)^2 J_1 \ll I_3,\ I_4 \ll I_1,\ I_2, \quad 0 \leqslant J_3/2 \leqslant J_4, \\ &J_3 = I_3 - 2(\chi I_2) J_1, \quad J_4 = I_4 - (\chi I_2) J_2. \end{aligned} \tag{74}$$

The resultant phase sequence is shown in Fig. 15 and has the following character: In the region of weak magnetic fields, a sequence of first-order transition proceeds and terminates at the phase (2, 2):

$$(2^2, 1^2) \to (2^4, 1^2) \to (2^6, 1^2) \to \ldots \to (2^{2m}, 1^2) \to \ldots \to (2,2).$$

This sequence is surprisingly similar to the experimental phase diagram obtained for CeSb in Refs. 1–3 (see, e.g., the phase diagrams in Refs. 3 and 5).

The free energy of the sequence of these phases, as a function of the parameter ξ at $h = 0$, is shown in Fig. 16. The same figure shows a plot of the free energy of the magnetic phase $(2, 1)\uparrow$. This plot is parallel to the analogous plot for the phase $(2^2, 1^2)$. With increasing magnetic field, the free energy of the phase (2, 1) decreases. Thus, with increasing field, the phase $(2^2, 1^2)$ vanishes first, next $(2^4, 1^2)$, etc. In addition, the degeneracy line of the phases (2, 2) and $(2, 1)\uparrow$ splits, with formation of a sequence of magnetic phases $(2^3, 1)\uparrow$, $(2^5, 1)\uparrow$, etc. With further increase of the magnetic field, the phase transition proceeds approximately as near the $F\uparrow - (2, 1)\uparrow$ degeneracy line on Fig. 8. If the inequalities (74) hold, the topological phase sequence agrees well with experiment. The phase diagram plotted in the variables χ and h is shown in Fig. 15(a). On changing to the variables T and h, the

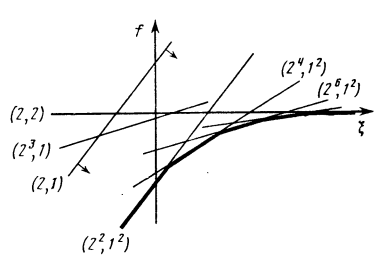

FIG. 16.

diagrams becomes greatly deformed, since the susceptibility $\chi(T)$ changes quite rapidly when T is close to T_c, and relatively slowly at low temperatures. The regions where the high temperature phases exist become therefore narrower on the phase diagram plotted in the variables T and h [Fig. 15(b)], and those with the low temperature phases broaden considerably, in agreement with the experiment. Comparing the experimental phase diagram of CeSb with that obtained in our approach, we obtain estimates of I_1, I_2, and I_0. The later can be obtained by expressing it in terms of the transition temperature with the aid of the Kramers-Wannier relation

$$\mathrm{sh}\,(2I_0/T_c)=1.$$

According to experiment, $T_c \approx 16$ K, hence $I_0 \approx 7$ K. The values of I_1 and I_2 can be obtained from the values of the magnetic field corresponding to the $(2,1)\uparrow - F\uparrow$ transition. According to this theory this value is

$$H_1=2(I_1+I_2).$$

In the experiments, $H_1 \approx 35$ kOe. It is clear therefore that neither I_1 nor I_2 exceeds 0.5 K. The strong-anisotropy condition is thus well satisfied.

The modulated states were classified experimentally in accord with the wave vector of the Bragg reflection corresponding to the maximum intensity. These wave vectors k, measured in units of π/a (a is the lattice constant) agree with the analogous wave vector of the modulated structures obtained by us. Explanations are needed for the antiferromagnetic phase with $k=8/13$ and the ferromagnetic with $k=6/11$, observed in the experiments. According to our interpretation, they can be represented in the form

$$(2^4, 1^2, 2^4, 1^2, 2^2, 1^2) \quad (k={}^8/_{13}),$$
$$(3, 1, 3, 1, 2, 1)\uparrow \quad (k={}^6/_{11}).$$

It is possible that these phases result from an even finer splitting than accounted for in our theory.

A more careful comparison with the experimental data, however, reveals important discrepancies. The antiferromagnetic structures obtained by us in weak fields should have two Bragg reflections of comparable intensity, with wave vectors $(l+1)/(2l+1)$ and $l/(2l+1)$ in units of π/a [the period of the modulated structure is $2(2l+1)$]. Thus, for example, at $l=1$ (phase $k=2/3$) the ratio of these intensities is 3:1. At large l their intensity become equalized and the distance between them decreases. The reflection that follows the principal one differs from them in intensity by a factor 9. No reflection corresponding to $k=l/(2l+1)$ is observed in the experimentally investigated CeSb phases having l ranging from one to five.

The possible cause of this discrepancy is the crude model used by us. In a real situation cubic anisotropy leads to the roughest splitting of the magnetic level with $J=5/2$ into a quartet and a doublet. The description of this situation with the aid of the usual Ising model is a rough qualitative approximation. One can hardly take too seriously the Bragg-reflection intensities obtained within the framework of this model. We hope, however, that the main feature, and particularly the topological structure, will remain the same when a more realistic account is taken of the interactions.

In the interpretation of a structure experiment on cerium antimonide it was proposed in Refs. 1–3 that certain planes are paramagnetic. This assumption seems to us to contradict the reliably established fact of the layered magnetic structure. Indeed, if the interplanar bonds can be regarded as week, then the ferromagnetic state of each plane changes into paramagnetic at a perfectly defined temperature. If, however, account is taken of the interaction between the planes, the fluctuations become three-dimensional near the phase-transition temperature. It is therefore utterly impossible to observe individual paramagnetic planes.

There exists also another cerium compound, CeBi, whose magnetic structure is also quite complicated.[13,14] The phase diagram of CeBi can apparently be interpreted with the aid of the method employed by us. A preliminary analysis shows, however, that we are dealing here with another range of values of the parameters. A detailed analysis of the magnetic structure of CeBi will be presented in another paper.

We thank D. I. Khomskiĭ for pointing out the experiments[13,14] on CeBi.

[1)]Cerium antimonide CeSb has an NaCl-type lattice. Its strong anisotropy is presently assumed (see Refs. 5–7) to be due to two factors, the Jahn-Teller effect and the proximity of the localized $4f$ electron to the Fermi surface. Small lattice deformations lead in this situation to strong changes of the electron wave function.

[2)]To prevent confusion, the quantities with respect to which the free energy is minimized (p, r, and s in this case) are called variables. The remaining quantities on which the free energy depends, such as ξ, are called parameters.

[3)]We present no proof of this statement. It can be obtained by mathematical induction and is straightforward albeit cumbersome. The last stages of the proofs will be omitted also in the sections that follows.

[1]J. Rossat-Mignod, P. Burlet, J. Villain, H. Bartholin, Tcheng-Si Wang, D. Florence, and O. Vogt, Phys. Rev. **B16**, 440 (1977).
[2]P. Fischer, B. Lebech, G. Meier, B. D. Rainford, and O. Vogt, J. Phys. **C11**, 345 (1978).
[3]G. Meier, P. Fischer, W. Haig, B. Lebech, B. D. Rainford, and O. Vogt, *ibid.* **C11**, 1172 (1978).
[4]B. Lebech, K. Clausen, and O. Vogt, *ibid.* **C13**, 1725 (1980).
[5]J. Rossat-Mignod, P. Burlet, H. Bartholin, O. Vogt, and R. Lagnier, *ibid.* **C13**, 6381 (1980).
[6]B. Coqblin and J. R. Schrieffer, Phys. Rev. **185**, 847 (1969).
[7]R. Siemann and B. R. Cooper, *ibid.* **B19**, 2645 (1979).
[8]P. Bak and J. von Boehm, *ibid.* **B21**, 5297 (1980).
[9]W. Selke and M. E. Fisher, *ibid.* **B20**, 257 (1979).
[10]M. E. Fisher and W. Selke, Phys. Rev. Lett. **44**, 1502 (1980).
[11]G. S. Parry, Mater, Sci. Eng. **31**, 99 (1977).
[12]D. E. Moncton, F. J. DiSalvo, J. D. Axe, L. J. Sham, and B. R. Patton, Phys. Rev. **B14**, 3432 (1976).
[13]H. Bartholin, D. Florence, Tcheng-Si Wang, and O. Vogt, Phys. Stat. Sol. (a), **24**, 631 (1974).
[14]H. Bartholin, P. Burlet, S. Quezel, J. Rossat-Mignod, and O. Vogt, J. de Phys. **40**, Colloq. C5, 130 (1979).

Translated by J. G. Adashko